



Kinetic and thermodynamic studies of malachite green adsorption on alumina

M. Aazza, H. Moussout, R. Marzouk, H. Ahlafi*

*Laboratory of chemistry and biology applied to the environment. Faculty of Sciences.
University My Ismail BP 11201-Zitoune. Meknes. 50000. Morocco.*

Received 9 Jan 2017
Revised 21 Mar 2017
Accepted 22 Mar 2017

Keywords

- ✓ Adsorption,
- ✓ Malachite Green,
- ✓ Alumina,
- ✓ Kinetic,
- ✓ Isotherm,
- ✓ Mechanism.

Abstract

The present study concerns the optimization of the parameters involved in the adsorption process of malachite green (MG) onto commercial alumina (Al_2O_3). The effect of temperature, pH, contact time (t_a) and initial concentration (C_0) of adsorbate on adsorbed amount was studied. It has been found that the retention rate of MG, by a mass $m = 0.1$ g of Al_2O_3 , is optimal by adopting the following experimental parameters: $\text{pH} = 7$, $C_0 = 8 \times 10^{-5}$ M and $t_a = 2$ h. The adsorption capacities (q_t), obtained at different adsorption temperatures (25, 30 and 40 °C), are respectively equal to 13.49, 13.61 and 13.64 mg/g. The modelling of the experimental results showed that the adsorption kinetics of MG on Al_2O_3 follow pseudo-second-order kinetics at the temperatures studied, while the Langmuir model describes the adsorption isotherms. The thermodynamic study showed that the adsorption reaction of MG on Al_2O_3 is spontaneous ($\Delta G^\circ < 0$) and endothermic ($\Delta H^\circ > 0$). The characterization of surface of alumina by FTIR, XRD and DTA/TGA, before and after its contact with MG, made it possible to elucidate the nature of the interactions between MG and Al_2O_3 .

1. Introduction

Currently, the synthesis dyes constitute a real industry and a capital of modern chemistry. The structural diversity of synthetic dyes derives both from the diversity of the chromophoric groups which compose them (azo, anthraquinone, triarylmethane and phthalocyanine groups), and the diversity of the application technology (direct reactive staining). For example, the fabrics are made from coloured textile fibres using different dyes that give them the final colour. However, liquid emissions generated by various industries represent a serious threat to the neighbouring ecology due to the toxicity of this type of compounds, which directly threatens human health and the environment. Indeed, these synthetic dyes, present in industrial effluents, have the property of being non-degradable, stable to oxidizing agents and to radiation, which aggravates the contamination of surface water and groundwater. Their presence in water, even with infinitesimal quantities, modifies its flavour, colour and its smell, making it unfit for consumption. In addition, they are carcinogenic. It is for these reasons that it is necessary to find effective ways for the abatement of these dyes before their release to receiving environment. One of the most widely used dyes in the textile industry is the malachite green which is endowed with important cationic properties which offer it various uses, such as dyeing fabrics, leather, cotton, etc. It is also used in the food industry and as a bactericide, fungicide and disinfectant[1–3].

Initially, several techniques have been used for the treatment of this type of pollutants, among which membrane processes, ion exchange, chemical precipitation, etc. can be cited [4–6]. However, these methods have shown their limits, in particular, with regard to the rate of removal of the pollutant and the cost of its abatement. In contrast, the adsorption method[7] has become the most used methods due to its simplicity and cost, in particular when the adsorbent used is less expensive. In this sense, several natural adsorbents such as clays, biopolymers and solids derived from biomass have been used in the adsorption process for the elimination of both organic

and inorganic pollutants. A comparison of the adsorption capacities of different solids with respect to malachite green was published by Franklin Joseph et al. [8].

The objective of this study is to test another type of adsorbent for the treatment of liquid effluents charged with malachite green, in this case alumina. Indeed, alumina is a very abundant mineral compound in the earth's crust after silica. Its production from $\text{Al}(\text{OH})_3$ is very easy and is characterized by a very large surface area of BET, which is of general interest in the field of heterogeneous catalysis. The aim of this work is to study the kinetic and the isothermal adsorption of MG on Al_2O_3 by examining in particular the effect of pH, the initial concentration C_0 of MG, the adsorption temperature and the mass of alumina, on the capacity of its adsorption.

2. Materials and Methods

2.1. Materials

The cationic malachite green of the formula $(\text{C}_{23}\text{H}_{25}\text{N}_2)_2(\text{HC}_2\text{O}_4)_2 \cdot \text{H}_2\text{C}_2\text{O}_4$ is known from the International Union of Pure and Applied Chemistry (IUPAC) under the nomenclature of 4-[(4-dimethylaminophenyl)-phenyl-methyl]-N, N-dimethylaniline. The $\gamma\text{-Al}_2\text{O}_3$ (93% of purity) with BET surface area of $103 \text{ m}^2/\text{g}$ is used as adsorbent for malachite green. These products are purchased from Lobachemie, India.

2.2. Methods

The kinetics and the adsorption isotherms were carried out in static mode at different temperatures. A mass m (g) of Al_2O_3 is impregnated with $V_{\text{sol}} = 20$ ml of malachite green solution (initial concentration $C_0 = 8 \times 10^{-5} \text{ mol/L}$). Thereafter, resulting suspension is well mixed (4500 rpm) for a predetermined period t_a of adsorption. After each time t_a , the solid is separated from the solution by a vacuum filtration system, using a $0.45 \mu\text{m}$ membrane. The resulting filtrate, which contains the residual concentration C_e of MG, was analysed by UV/Visible and the solid recovered after contact with MG is analysed by IRTF, XRD and DTA/GTA. The amount of the adsorbed MG on the alumina is calculated by the following relation:

$$q_t = \frac{C_0 - C_e}{m} \times V_{\text{sol}} \quad (1)$$

Where q_t represents the adsorption capacity (mg/g). C_0 and C_e are the concentrations, respectively, of MG, before and after adsorption.

C_0 and C_e are determined by UV/visible spectrophotometry, following the intensity of evolution of the more intense MG absorption band, located at $\lambda_{\text{max}} = 618 \text{ nm}$. The effect of the pH solution on the adsorption of MG is tested in a pH range between 4 and 12. The maximum adsorption capacity is determined from the plot of the adsorption isotherms obtained in a concentration range of MG between $C_0 = 4 \times 10^{-6} \text{ M}$ and $6 \times 10^{-5} \text{ M}$.

2.3. Characterisation techniques

UV/visible spectrophotometer (UV mini-1240; Brand Shimadzu) was used for MG concentration determinations before and after its adsorption at $\lambda_{\text{max}} = 618 \text{ nm}$. The calibration curve of Beer Lambert ($A = \epsilon \cdot L \cdot C$) was linear in the range of the concentrations used with excellent correlation coefficient. X-ray Diffraction (XRD), Fourier Transform Infrared spectroscopy (FTIR) and Differential Thermal/Thermogravimetric Analysis (DTA/TGA) were used to characterize the solid phase of adsorbent. These techniques allow us to elucidate the nature of the interactions which can occur between MG and alumina during the adsorption process.

3. Results and discussion

3.1. Characterisation of alumina and MG

3.1.1. FTIR

The FTIR spectrum of commercial alumina is shown in figure 1 (Spectrum a). The two intense bands, located between 1000 and 500 cm^{-1} are characteristics of the frequency vibrations of the Al-O bonds in octahedral (AlO_4) and tetrahedral (AlO_6) geometries in alumina [9,10]. The band at 3450 cm^{-1} corresponds to the stretching vibration of OH groups in Al-OH and the physisorbed H_2O , which give the deformation bands at 1651 cm^{-1} . The spectrum d, represents the characteristic IR bands recorded for MG. Table 1 summarizes the different bands observed and their attributions.

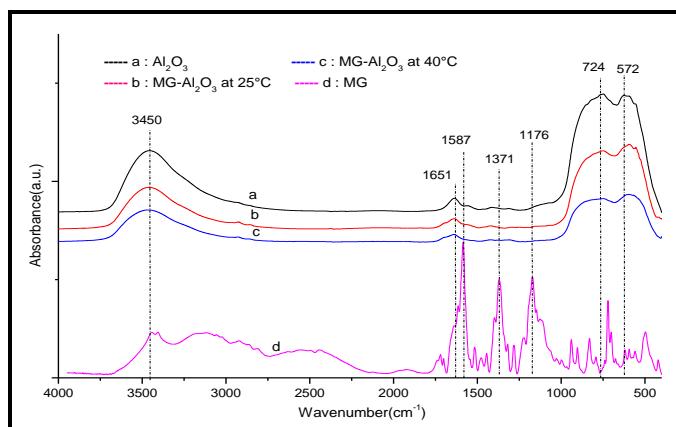


Figure 1: FTIR spectra of Al₂O₃ (a), MG (d) and MG-Al₂O₃ (b, c).

Table1: Attribution of IR bands of MG.

Bands (cm ⁻¹)	Attributions
1615 – 1585	Stretching C=C aromatic
1370	Stretching C-C aromatic
1175	Stretching C-N
3400 ; 3452	Stretching O-H
3000-3250	Stretching N-H
2800 – 2900	Stretching C-H

3.1.2. DTA/TGA

Figure 2 shows the DTA/TGA curves of Al₂O₃ (Figure 2, spectrum a) and MG (Figure 2, spectrum b), recorded between 25 and 600°C with heating rate $\beta = 20$ °C/min. In the case of alumina, a single endothermic peak at 109 °C is observed, it corresponds to a mass loss of (-11.7%), attributed to H₂O physisorbed on the of alumina surface. A second broad endothermic peak located between 450 and 650 °C, is linked to the deshydroxylation of alumina at high temperature. In the thermogram of MG there are four peaks, located respectively, at 223.15, 294.26, 514.14 and 547.20°C, with a loss of the total mass of -80%. These peaks correspond to the decomposition/degradation of MG and its oxidation at high temperatures (exothermic peak at 547 °C).

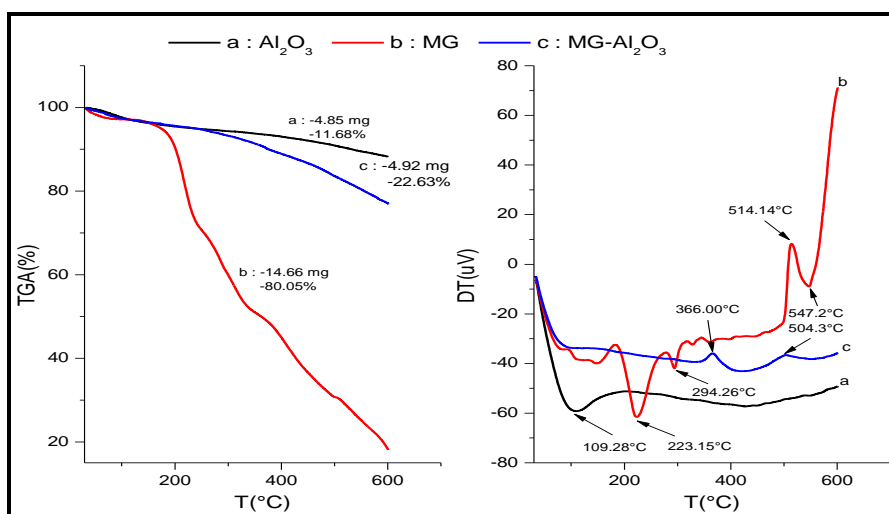


Figure 2: DTA and TGA of Al₂O₃ (a), MG (b) and MG-Al₂O₃ (c)

3.2. Study of adsorption kinetics of MG onto Al₂O₃

3.2.1. Effect of pH on MG removal

The pH of the solution is an important parameter which has an influence both on the charges of the adsorbent surface and the degree of ionization of the MG dye and consequently on the adsorption process. As well, the pH effect on effectiveness of elimination of MG has been studied at different pH. The initial pH of the solution is

adjusted by the addition of HCl (0.1 M) or NaOH (0.1 M) to obtain a desired value of pH between 4 and 11. Figure 3.a gives the evolution of an adsorbed quantity of MG onto alumina at different pH of the solution. This curve shows that the adsorption of MG is favoured at basic pH, higher than pH = 6. Below this value of pH, the amount adsorbed is low. A similar result has been obtained by other authors using the silica as an adsorbent[11,12].Indeed, in basic medium the charge of alumina surface is negative and in acid medium its charge is positive because the point of zero charge of alumina is determined at pH = 6 [13]. At this pH, the MG is present under its cationic form, which promotes its interaction with the negative charges of alumina. For lower pH < 6, the protonation of hydroxyl groups of alumina led to repulsion of cationic MG, which explains the decrease of the amount adsorbed at acidic pH. For pH > 7, the MG exists in its basic form containing a carbinol groups.

3.2.2. Effect of initial mass of the alumina

This study was conducted by using different mass of alumina (m = 0.1, 0.2 and 0.3 g). The obtained results are shown in figure 3.b. It can be found for $t_a < 30$ min of contact time, a progressive increase of the amount of adsorbed MG with a mass of alumina, and at the same time the adsorption kinetics was very fast, due to the availability of adsorption sites. For > 60 min, the amount adsorbed stabilizes, indicating the establishment of the equilibrium between the adsorbed phase and the residual concentration. Therefore, the optimum mass used has been fixed to m = 0.1 g.

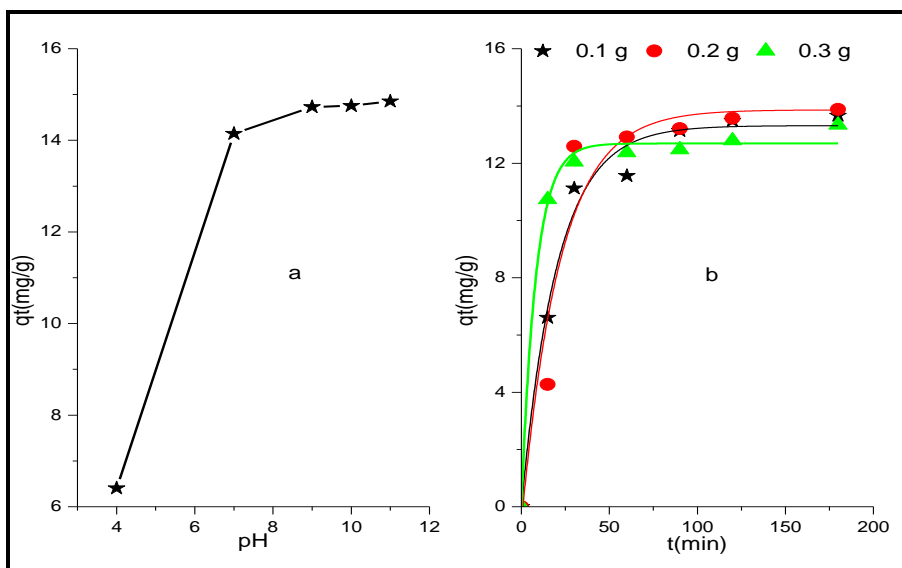


Figure 3: pH (a) and mass (b) effects of Al₂O₃ on adsorption of MG.

3.2.3. Effect of temperature on MG removal

The adsorption kinetics can provide more information about the mechanism of adsorption and transfer mode of MG from liquid phase to the solid phase. The literature reports a number of kinetic models of adsorption which have been proposed by Kannan et al., Lagergren et al. and Ho et al.[14,15]. In order to analyse the adsorption rate of MG on Al₂O₃ at different temperatures, both the pseudo first order kinetic (Equation (2) and (3)) and the pseudo second order kinetic models (Equation (4)) have been used as follows:

$$\ln(q_e - q_t) = \ln(q_e) - k_1 t \quad (2)$$

$$\frac{1}{q_t} = \frac{k_1}{q_e} \frac{1}{t} + \frac{1}{q_e} \quad (3)$$

$$\frac{t}{q_t} = \frac{1}{k_2 q_e^2} + \frac{t}{q_e} \quad (4)$$

Where q_e and q_t are the adsorbed quantities of MG (mg/g) at equilibrium and desired times, respectively. k_1 , k_1' (min^{-1}) and k_2 ($\text{g/mg} \cdot \text{min}$) are the pseudo-first and the pseudo-second rate constants, respectively.

According to figure 4 it can be seen that the adsorption kinetics of MG on Al₂O₃ at different temperatures is initially very fast, then stabilises from $t_a = 60$ min of contact time that represents the equilibrium time of

adsorption at studied temperatures. Thus, the contact time $t_a = 2\text{h}$ is considered for the study of adsorption isotherms of MG on Al_2O_3 . At saturation of solid surface, the amount adsorbed is 13.49, 13.61 and 13.64 mg/g, respectively, for $T = 25, 30,$ and $40\text{ }^\circ\text{C}$. To examine the adsorption mechanism, we evaluated a pseudo-first-order and a pseudo-second-order kinetic model to determine which model shows the best fit with the experimental data. This was done by comparing the experimental curves (Figure 4) with the equations of the previous models. From figure 5, it appears obvious that the adsorption kinetics of MG on Al_2O_3 follows the pseudo second order kinetic for the temperatures studied, since the experimental points are well represented by this model. In addition, according to table 2, the regression coefficients R^2 are close to 1 and the adsorbed quantities, calculated from this model, are close to those determined experimentally for the three temperatures.

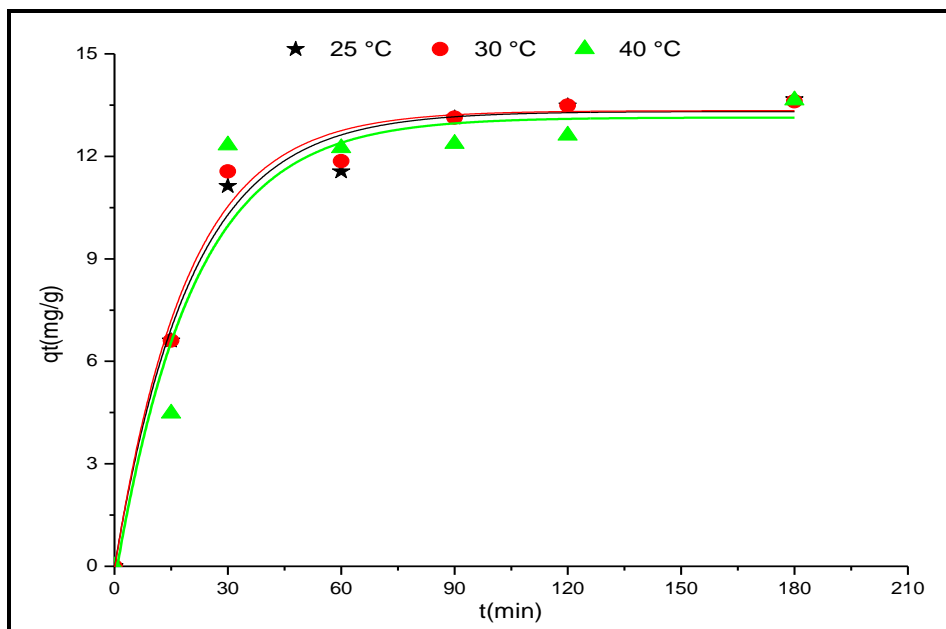


Figure 4: Adsorption kinetics of MG onto Al_2O_3 at different temperatures.

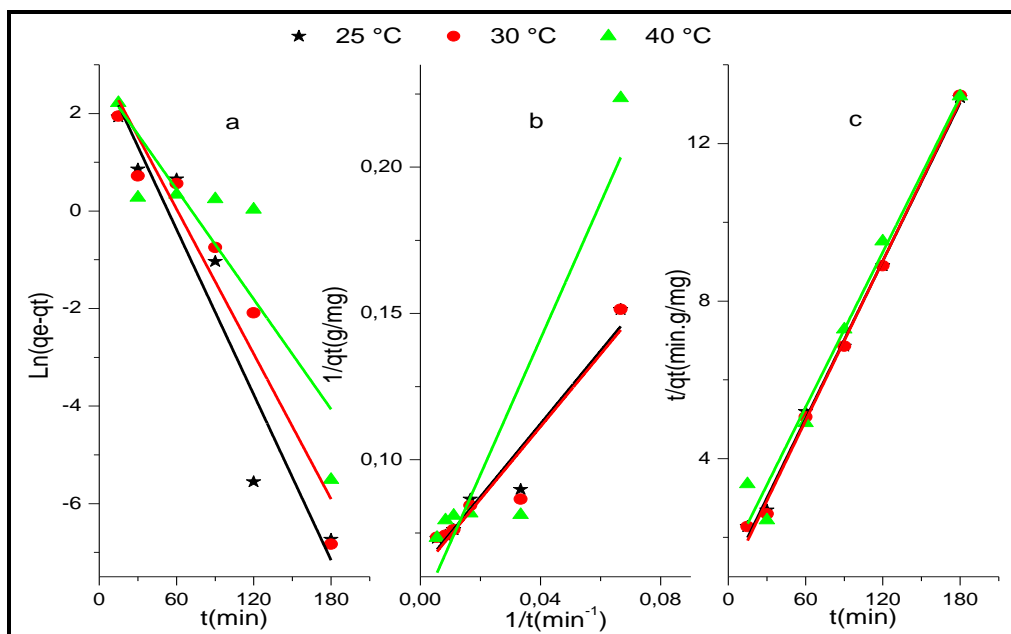


Figure 5: Pseudo first order (a, b) and pseudo second order (c) kinetic models for adsorption of MG on Al_2O_3 at different temperatures.

Table 2: Parameters of adsorption kinetic models of MG on Al_2O_3 .

T (°C)	Lagergren				Kannan			Ho et Coll		
	q_{exp} (mg/g)	k_1 (min ⁻¹)	q_e (mg/g)	R_1^2	k_1' (min ⁻¹)	q_e (mg/g)	R_2^2	k_2 (g/mg.min)	q_e (mg/g)	R_2^2
25	13.490	0.057	20.488	0.955	20.000	16.030	0.971	3.81×10^{-3}	14.941	0.998
30	13.610	0.050	20.455	0.968	20.078	16.200	0.960	4.16×10^{-3}	14.778	0.998
40	13.640	0.038	14.869	0.876	47.933	20.631	0.917	5.64×10^{-3}	14.520	0.987

3.2.4. Activation energy

The activation energy (E_a) of adsorption of MG on Al_2O_3 can be calculated from the kinetic data, obtained at different temperatures. Especially, the rate constant of the pseudo second order model allowed to calculate E_a using the relationship of Arrhenius:

$$\ln(k_2) = \ln(A) - \frac{E_a}{RT} \quad (5)$$

With: k_2 is the rate constant of pseudo second order model (g/mg.min), A is the pre-exponential factor (g/mg.min), E_a is the activation energy (kJ/mol), R is the gas constant (8.314 J/mol.K) and T is the temperature of adsorption (K).

Figure 6 gives the right obtained whose slope leads to a value of $E_a = 20.80$ kJ/mol, and intercept to $A = 16.496$ g/mg.min. The value of E_a , involved in the adsorption of MG on Al_2O_3 is less than 40 kJ/mol, which indicates the existence of a barrier of relatively low energy, characteristic of physical adsorption.

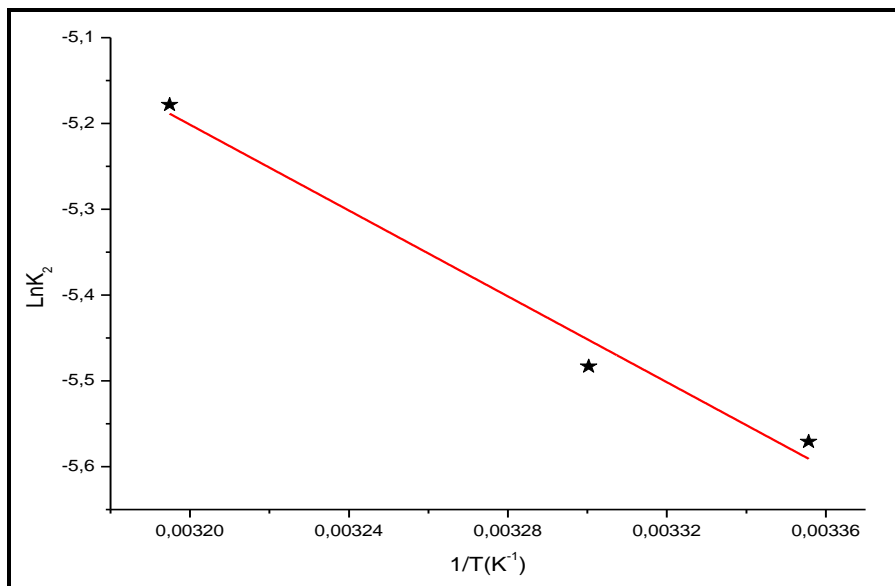


Figure 6: Plot of Arrhenius equation for adsorption of MG on Al_2O_3 .

3.3. Adsorption isotherms

The adsorption isotherms of MG on alumina are represented by the adsorbed amount versus residual concentration of MG at different temperatures of adsorption. The experimental isotherms obtained are shown in figure 7. These isotherms have been confronted to Langmuir and Freundlich models[16,17], whose equations are the following:

- Langmuir model[16]: The Langmuir equation is established for a surface of solid with uniform sites and without interactions between adsorbed species, either:

$$q_e = \frac{q_m K_L C_e}{1 + K_L C_e} \quad (6)$$

With: q_m (mg/g): maximum amount of MG adsorbed, q_e (mg/g): equilibrium amount of MG, K_L (L/mg): Langmuir constant and C_e (mg/L): residual concentration of solute at equilibrium.

- Freundlich model[17]: Unlike Langmuir model, the Freundlich model is based on assumption that the adsorption sites of solid are heterogeneous with different activation energies, either:

$$q_e = K_F C_e^{1/n} \quad (7)$$

With: K_F ($\text{mg}^{(1-n)} \cdot \text{L}^n \cdot \text{g}^{-1}$): Freundlich constant and n : Freundlich constant associated to the affinity between adsorbate and adsorbent.

Figure 7 shows the theoretical curves, plotted using the non-linear expressions of the above equations. It may be noticed that the curves issued from the Langmuir model, properly follow the experimental isotherms curves for the three adsorption temperatures. This indicates that the adsorption of MG on Al_2O_3 is done on homogeneous sites forming a molecular monolayer. Indeed, the values of correlation coefficients R^2 (Table 3) are higher in the case of Langmuir model, in good agreement with the previous conclusion. In addition, the maximum quantities of pollutant adsorption (q_m) are comparable to those found experimentally for each adsorption temperature. It may be observed also that the temperature does not have a significant effect on the amount of MG adsorbed on alumina.

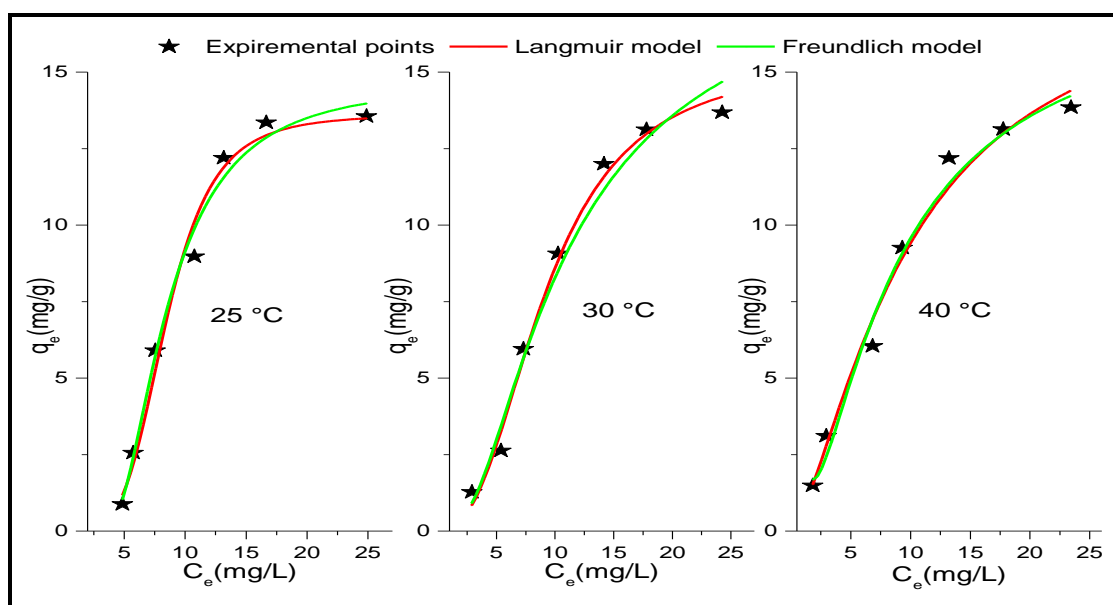


Figure 7: Adsorption isotherms of MG on Al_2O_3 fitted with nonlinear models of Langmuir and Freundlich.

Table 3: Parameters of nonlinear models of adsorption isotherms of MG on Al_2O_3 .

T (°C)	Langmuir			Freundlich		
	q_m (mg/g)	K_L (L/mg)	R^2	$1/n$	K_F ($\text{mg}^{(1-n)} \text{L}^n \text{g}^{-1}$)	R^2
25	13.611	1.0×10^{-4}	0.988	0.020	14.630	0.989
30	15.417	4.0×10^{-3}	0.988	0.059	19.128	0.981
40	18.406	3.7×10^{-2}	0.990	0.100	20.067	0.986

3.4. Thermodynamic Study

The thermodynamic quantities such as free energy (ΔG°), enthalpy (ΔH°) and entropy (ΔS°) have been determined by the exploitation of previous experiences, using the relationship of Van't Hoff, either:

$$\Delta G^\circ = -RT \ln K_c = \Delta H^\circ - T\Delta S^\circ \quad (8)$$

$$\ln K_c = -\frac{\Delta H^\circ}{RT} + \frac{\Delta S^\circ}{R} \quad (9)$$

Where

$$K_c = \frac{C_{ads}}{C_e}$$

The plot of $\ln(K_c)$ versus $1/T$ (Figure 8) displays a linear curve, where the slope and intercept allow to calculate respectively, the values of ΔH° , ΔS° and ΔG° . Table 4 shows that the free energy is negative, which suggests a spontaneous adsorption of MG on Al_2O_3 . The positive values of ΔH° and ΔS° confirm, respectively, the endothermic character of the reaction and an increase in the degrees of freedom at the liquid/solid interface.

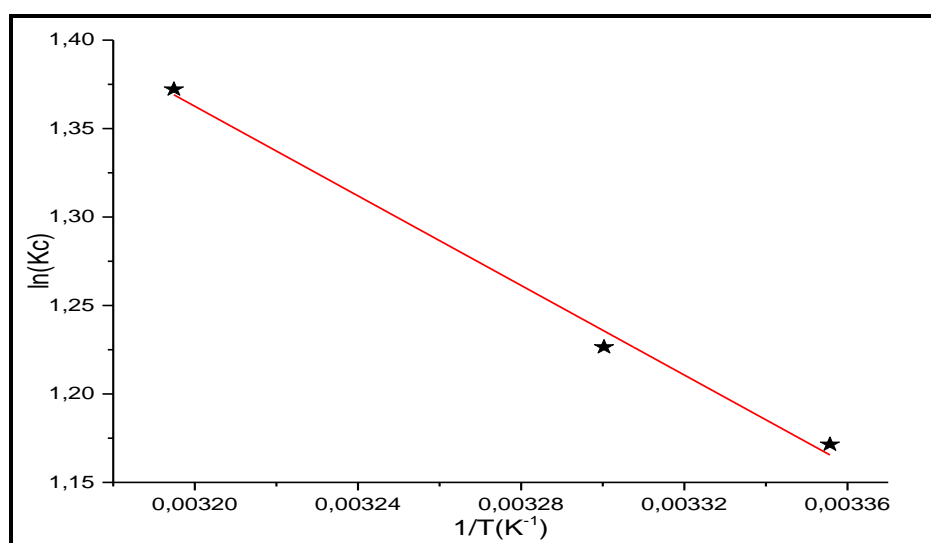


Figure8: Plot of $\ln K_c$ versus $1/T$.

Table4: Thermodynamic parameters for the adsorption of MG on Al_2O_3 .

T (°C)	R ²	ΔS° (J/K, mol)	ΔH° (kJ/mol)	ΔG° (kJ/mol)
25				-2.902
30	0.997	45.006	10.520	-3.090
40				-3.571

3.5. Adsorption mechanism of MG onto Al_2O_3

The characterisation of the alumina after its contact with MG is useful in the sense that it can provide information concerning the nature of the interactions that occur between MG and the adsorption sites. This characterisation was performed by FTIR, XRD and DTA/TGA techniques.

The analysis of alumina by FTIR before and after its contact with MG led to the spectra of the figure 1 for the adsorption temperatures considered ($T = 25$ and 40 °C). By comparison with the spectrum of alumina, it can be found a significant decrease of intensities of the bands related to O-H and Al-O groups of alumina (3450 , 1651 , 724 and 572 cm^{-1}). These decreases are due to a strong interaction of these groups with MG. In addition, the intensity of band at 724 cm^{-1} (Al-O-Al) decreases faster than that of the band at 572 cm^{-1} (Al-O), which indicates a stronger interaction of this group with MG. The same developments have been observed by different authors, using various adsorbents, for the removal of MG [11,12,18,19]. Overall, these changes have been attributed to electrostatic interactions between the cationic groups ($-N^+$) of MG and the negatively charged groups ($-Al-O^-$) on alumina surface. Kannan et al.[12] indicate that these interactions also occur between the free doublet of nitrogen atom in MG and Al atom, according to Lewis theory of donor/acceptor: $Al \leftarrow N$. However, Y.C.Lee et al.[19] indicate that for $pH > 7$, the carbinol group of basic form of MG is at origin of interaction between MG and clay modified by aminopropyl.

In addition, the analysis of the same samples by XRD also shows a net decrease in the intensities of peaks recorded after adsorption of MG on alumina (Figure 9). The disappearance of peak at $2\theta = 32^\circ$ indicates that the orientation of alumina plans is no longer retained because of its interaction with MG. Similar results have been mentioned by Y,C, Lee et al.[19] with adsorption of MG on phyllosilicate magnesium.

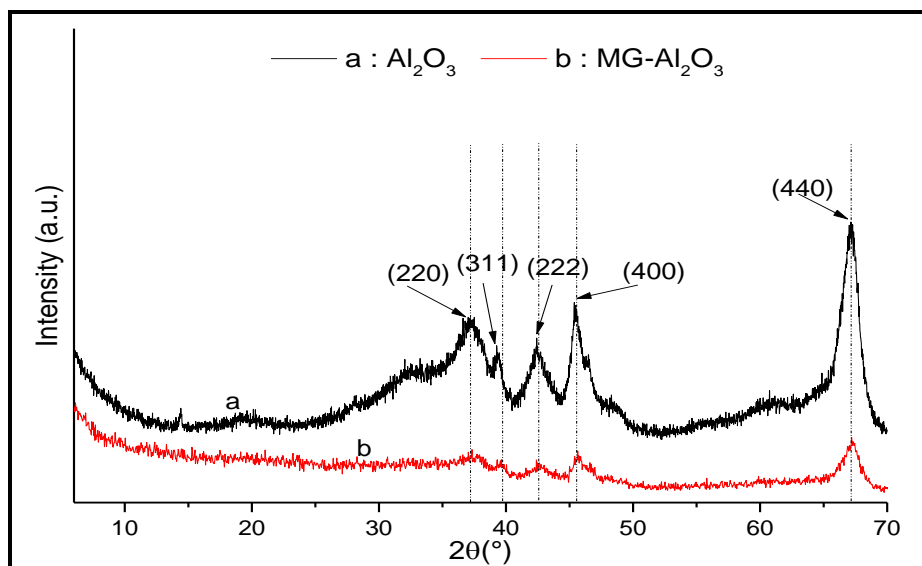


Figure 9: XRD patterns of Al_2O_3 and $\text{MG-Al}_2\text{O}_3$.

Previous changes have been confirmed by DTA/TGA analysis whose thermograms are represented in Figure 2. The loss of mass observed between 25 and 600 °C, for the solid $\text{MG-Al}_2\text{O}_3$ is -22.6%, higher than the one obtained in the case of alumina (-11.7%) and less than of that of MG (-80%) alone, which reflects a gain in thermal stability of MG, which justifies its interactions with alumina in the course of adsorption reaction. This characteristic is similar to that generally observed in the case of composite materials. In the DTA curve of $\text{MG-Al}_2\text{O}_3$, two exothermic peaks are recorded at 366 and 504 °C unlike the DTA peaks of Al_2O_3 and MG analysed individually (Figure 2). In the case of MG, the endothermic peaks located at 223 and 294 °C do not appear on the thermogram of $\text{MG-Al}_2\text{O}_3$ sample. The presence of these peaks indicates that the degradation reactions of MG under air were modified due to its interaction with Al_2O_3 . As well, these two peaks are attributed to the thermal degradation and oxidation of MG adsorbed on alumina, which is in conformity with the loss of mass observed (22.6%), which is due in large part to these two phenomena [20].

Conclusion

The use of commercial alumina for the removal of MG from wastewater has given very satisfactory results and can constitute an alternative to other adsorbents. The results show that the adsorption of this effluent is influenced by several factors (pH, C_0 , m and T). The rate of adsorption increases with the increase of contact time and a decrease of the adsorption temperature. The optimum values of pH and mass of adsorbent are respectively equal to 7 and 0.1 g at ambient temperature. The adsorption kinetic of MG at different temperatures was described by the pseudo second order model and the adsorption isotherms of MG on alumina are consistent with the Langmuir model. The value of activation energy shows that the interactions between MG and alumina correspond to physisorption. The thermodynamic study shows that the adsorption reaction is endothermic and spontaneous.

The characterisation of alumina, before and after its contact with MG, by FTIR, XRD and DTA/TGA, has allowed to elucidate the interactions between adsorbate and adsorbent.

References

1. Méndez A., Fernández F., Gascó G., *Desalination*. 206 (2007) 147–153. doi:10.1016/j.desal.2006.03.564.
2. Gupta V.K., Mittal A., Krishnan L., Gajbe V., *Sep. Purif. Technol.* 40 (2004) 87–96. doi:10.1016/j.seppur.2004.01.008.
3. Liu P.J., Hsieh W.T., Huang S.H., Liao H.F., Chiang B.H., *Exp. Hematol.* 38 (2010) 437–445. doi:10.1016/j.exphem.2010.03.012.
4. Kaminski W., Modrzejewska Z., *Sep. Sci. Technol.* 32 (1997) 2659–2668. doi:10.1080/01496399708006962.
5. Aldrich C., Feng D., *Miner. Eng.* 13 (2000) 1129–1138. doi:10.1016/S0892-6875(00)00096-0.
6. Erdem E., Karapinar N., Donat R., *J. Colloid Interface Sci.* 280 (2004) 309–314. doi:10.1016/j.jcis.2004.08.028.

7. Järup L., Br. *Med. Bull.* 68 (2003) 167–182. doi:10.1093/bmb/ldg032.
8. Joseph F., Agrawal Y.K., Rawtani D., *Front. Life Sci.* 7 (2013) 99–111. doi:10.1080/21553769.2013.803210.
9. Thabet M.S., Ismaiel A.M., *J. Encapsulation Adsorpt. Sci.* 6 (2016) 70–90. doi:10.4236/jeas.2016.63007.
10. Li J., Pan Y., Xiang C., Guo Q. Ge, J., *Ceram. Int.* 32 (2006) 587–591. doi:10.1016/j.ceramint.2005.04.015.
11. Tang H., Zhou W., Zhang L., *J. Hazard. Mater.* 209–210 (2012) 218–225. doi:10.1016/j.jhazmat.2012.01.010.
12. Kannan C., Sundaram T., Palvannan T., *J. Hazard. Mater.* 157 (2008) 137–145. doi:10.1016/j.jhazmat.2007.12.116.
13. Wawrzkiwicz M., Wiśniewska M., Gun'ko V.M., Zarko V.I., *Powder Technol.* 278 (2015) 306–315. doi:10.1016/j.powtec.2015.03.035.
14. Lagergren B.K.S.S. Zur theorie der sogenannten adsorption gelöster stoffe, *Veternskapsakad Handlingar*, 24 (1898) 1–39.
15. Ho Y.S., McKay G., *Chem. Eng. J.* 70 (1998) 115–124.
16. Langmuir I., *J. Am. Chem. Soc.* 40 (1918) 1361–1403. doi:10.1021/ja02242a004.
17. Freundlich H., Heller W., *J. Am. Chem. Soc.* 301 (1939) 2228–2230. doi:10.1021/ja01877a071.
18. Xu R., Jia M., Zhang Y., Li F., *Microporous Mesoporous Mater.* 149 (2012) 111–118. doi:10.1016/j.micromeso.2011.08.024.
19. Lee Y.C., Kim E.J., Yang J.W., Shin H.J., *J. Hazard. Mater.* 192 (2011) 62–70. doi:10.1016/j.jhazmat.2011.04.094.
20. Das A.K., Saha S., Pal A., Maji S.K., *J. Environ. Sci. Heal. Part A Toxic/Hazardous Subst. Environ. Eng.* 44 (2009) 896–905. doi:10.1080/10934520902958708.

(2017) ; <http://www.jmaterenvirosci.com>